ISSN 0006-2979, Biochemistry (Moscow), 2011, Vol. 76, No. 6, pp. 666-676. © Pleiades Publishing, Ltd., 2011.
Published in Russian in Biokhimiya, 2011, Vol. 76, No. 6, pp. 816-828.

Expression, Purification, and Characterization of Putative *Candida albicans* Rad3, the Product of *orf19.7119*

Ki Moon Seong[1,2#], Se Hyun Lee[1#], Hag Dong Kim[1], Chang Hoon Lee[3], Hyesook Youn[4], BuHyun Youn[5]*, and Joon Kim[1]*

[1]*School of Life Sciences and Biotechnology and BioInstitute, Korea University, Seoul 136-713, Korea; E-mail: joonkim@korea.ac.kr*
[2]*Present address: Radiation Health Research Institute, Korea Hydro and Nuclear Power Co., Ltd., Seoul 132-703, Korea*
[3]*Department of Polymer Science and Engineering, Chosun University, Gwangju 501-759, Korea*
[4]*Department of Bioscience and Biotechnology/Institute of Bioscience, Sejong University, Seoul, 143-747, Korea*
[5]*College of Natural Sciences, Department of Biological Sciences, Pusan National University, Pusan 609-735, Korea; E-mail: bhyoun72@pusan.ac.kr*

Received October 4, 2010
Revision received December 30, 2010

Abstract—Invasive infections of *Candida albicans* are life-threatening clinical conditions affecting immunosuppressed patients. To maintain genome integrity and diversity, *C. albicans* utilizes DNA repair systems, such as nucleotide excision repair (NER), to escape from attack by macrophages. Rad3 helicase is a component of the TFIIH complex, which plays a role in transcription and the NER pathway. Accumulated evidence of studies from Archaea to humans has revealed that the conserved structure, including an iron-containing domain, is essential in the function of Rad3 helicase activity. However, no study of the Rad3 protein of *C. albicans* has yet been reported. In the present study, putative *C. albicans* Rad3 (CaRad3) has been cloned with *orf19.7119* of the *Candida* genome. CaRad3 proteins were over-expressed and purified from *E. coli* and *S. cerevisiae* using a Ni-NTA column and a size exclusion column for physicochemical and functional characterization. Through EMR and spectrometric analysis, we have proven that the purified CaRad3 protein has a Fe-S cluster. We also revealed that CaRad3 protein has a helicase activity on a duplex DNA substrate. Furthermore, we showed that the CaRad3 protein purified from yeasts was N-glycosylated, and that this protein complemented the defects in both the NER pathway and transcription. These data suggest that the Rad3 helicase in *C. albicans* is the product of the *orf19.7119* gene.

DOI: 10.1134/S0006297911060071

Key words: *Candida albicans*, Rad3, DNA repair, Fe-S cluster, functional complementation

Xeroderma pigmentosum group D (XPD/ERCC2) is a representative helicase in the eukaryotic Rad3 family that displays 5′ to 3′ polarity of single strand DNA translocation [1]. Eukaryotic Rad3 (*H. sapiens* XPD, *S. cerevisiae* Rad3, *A. thaliana* Uvh6) protein is also a component of the transcription factor TFIIH complex, which plays a pivotal role in both the transcription initiation step of RNA polymerase II and the nucleotide excision repair (NER) pathway [2]. NER is an important cellular mechanism for maintenance of genome integrity, which is essential for survival of organisms by repair of most types of DNA lesions caused by exogenous agents [3-5]. The importance of NER in humans is underlined by the genetic disorders associated with defects in NER, namely xeroderma pigmentosum (XP), Cockayne syndrome (CS), and trichothiodystrophy (TTD) [6]. Central to understanding of these disorders is the *XPD* gene, mutations of which can result in XP, TTD, XP with CS, XP with TTD, and cerebro-oculofacial-skeletal syndrome (COFS), with wide variations in clinical features and severity [7-9]. XPD, together with XPB, supply opposite unwinding capacities required for local helix opening in formation of open DNA intermediates during NER [10]. However, a recent study demonstrated that the helicase activity of XPB is not used; the ATPase activity of XPB, in combination with the helicase activity of XPD, is used for opening of damaged DNA [11].

Thus, the helicase activity of XPD is exclusively utilized in NER. Functional point mutations in ATPase and

[#] These authors contributed equally to this work.
* To whom correspondence should be addressed.

helicase activities of XPD abolish NER activity, but not transcription, pointing to an important role of XPD in repair of damaged DNA [12]. Rad3 family helicases have a unique insertion containing iron-sulfur (Fe-S) clusters, which differ from the related SF2 (superfamily 2) enzymes. Fe-S clusters are ubiquitous and ancient prosthetic groups that are necessary for fundamental roles in structure and function. The Fe-S cluster in Rad3 helicase is essential in helicase for coupling of ATP hydrolysis to DNA translocation and for targeting to DNA [13]. *Candida albicans*, the single most important opportunistic fungal pathogen, makes good use of DNA repair systems in maintenance of genome integrity. *Candida albicans* exists as a commensal in the skin and mucosal surfaces of healthy individuals without causing disease. However, when the immune system of a host becomes debilitated or immunocompromised, *C. albicans* invades and colonizes host tissue, generating severe life-threatening systemic infection (candidaemia and deep-seated organ candidiasis) [14]. Upon *C. albicans* infection, innate immune cells, such as dendritic cells, macrophages, and neutrophils, rapidly produce reactive oxygen species (ROS) in the oxidative burst reaction, through assembly and activation of the nicotinamide adenine dinucleotide phosphate (NADPH) oxidase complex [15, 16]. A huge number of ROS molecules generated by the innate immune cells induces killing of invading pathogens. NER may play a role in development of systemic candidiasis, which requires survival of *C. albicans* cells upon attack of ROS by macrophages. The function of Rad3 protein in non-pathogenic *S. cerevisiae* (ScRad3) is well known through diverse genetic and biochemical approaches [2, 17-24]. However, a study for investigation of a counterpart of pathogenic *C. albicans* (CaRad3) has not yet been attempted. For analysis of the physical and functional properties of CaRad3 protein, isolation and characterization of the protein is essential. Bacterial expression systems are most commonly used for foreign protein production, since they are easy to handle, cost-effective, and easy to scale up; however, they lack a system of post-translational modification, such as that found in eukaryotes. Therefore, *S. cerevisiae* is a suitable eukaryotic system for expression and purification of *Candida* proteins in functional assays. In this study, we have cloned, overexpressed, and purified putative CaRad3 from *C. albicans*. We have also characterized the protein in terms of its structural, spectroscopic, and functional properties. The results indicate that the product of *orf19.7119* from the *C. albicans* genome is Rad3 (or XPD) of *C. albicans*, structurally and functionally.

MATERIALS ANS METHODS

Strains, plasmids, and media. *Escherichia coli* strain ER2566 (NEB Inc., USA) and plasmids pET21a (Novagen, USA), pESC(Ura) (Stratagene, USA), and pBluescript II KS(+) (Stratagene) were used for cloning of the *CaRad3* gene. *Escherichia coli* cells were cultured in LB medium (1% tryptone, 0.5% yeast extract, 0.5% sodium chloride) or modified YEP medium (2% peptone, 1% yeast extract, 0.2 M sorbitol). Where necessary, ampicillin (Invitrogen, USA) was added to the media at a final concentration of 100 μg/ml. For solid media, 2% agar was added to the media. *Saccharomyces cerevisiae* strains used in this study were kindly provided by Dr. S. Prakash and Dr. L. Prakash (University of Texas Medical Branch, Texas) and are described in the table. Standard genetic manipulation and transformation were used and standard yeast media, including YPD (1% yeast extract, 2% peptone, 2% dextrose) and synthetic complete media (0.67% yeast nitrogen base without amino acid, 2% dextrose), were prepared as previously described [25]. All other chemicals were of reagent grade and purchased from commercial sources.

Isolation of genomic DNA for *orf19.7119* from *C. albicans*. Cultured *C. albicans* BWP17 cells were harvested at A_{600} 1.0 and washed with chilled water. Cells were resuspended in lysis buffer (0.2 M Tris-HCl, pH 7.5, 0.01 M EDTA, 1% SDS, 0.5 M NaCl), and the same vol-

Candida albicans and *S. cerevisiae* strains used in this study

Strain	Genotype
C. albicans BWP17	*ura3Δ::λimm434/ura3 Δ::λimm434 his1::hisG/his1::hisG arg4::hisG/arg4::hisG*
S. cerevisiae BY4741	MATa *his3Δ1 leu2Δ0 met15Δ0 ura3Δ0*
DBY747	MATa *his3-Δ1 leu2–3,112 ura3–52 trp1–289 lys2–801*
YR3-19	DBY747 except for *rad3 Arg48*
RSY11	MATα *leu2–3,112 ura3–52 trp1 Δ can1*
YR3-57	RSY11 except for *rad3 Tyr590*

ume of TE buffer and phenol–chloroform–isoamyl alcohol (PCI) solution were added. Cells were broken with glass beads for 2 min using a FastPrep-24 apparatus (MP Biomedicals Products, USA). Extracts cleared by centrifugation at 13,000 rpm were mixed with absolute ethanol for ethanol precipitation. After washing with 70% ethanol, dried pellets were incubated with RNase A (10 mg/ml) at 37°C for 1 h. Genomic DNAs were retrieved from PCI and ethanol precipitation. Pellets were resuspended in sterilized distilled water.

Bacterial expression and purification of recombinant orf19.7119 protein. The *CaRad3* (putative *C. albicans Rad3*) gene was amplified from *C. albicans* BWP17 genomic DNA by PCR (forward: 5′-CCG CAA GGA TCC ATG AAG TTC TTT ATT GAC GAC-3′, reverse: 5′-ACA GTT CTC GAG CAA CAA ATC TAA ATC CTC CTC-3′), and the 2307 bp of PCR fragments were cloned into the pET21a vector (Novagen) using *Bam*HI/*Xho*I recognition sites for expression of C-terminal His-tagged recombination CaRad3 in *E. coli*. CaRad3 protein was expressed in ER2566 (NEB Inc.) cells and induced for 20 h at 15°C by addition of IPTG (0.1 mM). Cell pellets were resuspended in lysis buffer (50 mM NaH_2PO_4, 300 mM NaCl, 10 mM imidazole, pH 8.0, 2 mM β-mercaptoethanol, 10% glycerol), and lysed by sonication (5 × 10 sec, model 450 Sonifier; Branson Ultrasonics Co., USA). Crude extracts were cleared by centrifugation (20,000*g* for 40 min). Following centrifugation, the supernatant was incubated with nickel-nitrilotriacetic acid agarose (Qiagen, USA) for 1 h in an overhead shaker at 4°C. After washing with 20 column volumes of wash buffer (50 mM NaH_2PO_4, 300 mM NaCl, 20 mM imidazole, pH 8.0), the fusion protein was eluted stepwise with 50 mM NaH_2PO_4, 300 mM NaCl, and 100-500 mM imidazole, pH 8.0. Fractions containing CaRad3 protein were identified by SDS-PAGE, pooled by ultrafiltration in an Amicon 8050 cell with a 30 kDa cutoff membrane (Millipore, USA), and purified to homogeneity using a Superdex G-100 size exclusion column (2 × 100 cm) equilibrated with gel filtration buffer (20 mM Tris-HCl, pH 8.5). Purified CaRad3 proteins were concentrated by ultrafiltration in an Amicon 8050 cell with a 10 kDa cutoff membrane (Millipore) with a final purity of >99%, as estimated by SDS-PAGE (Coomassie Brilliant Blue staining), and the concentrations were determined using the Bradford method.

Expression and purification for the product of *orf19.7119* in *S. cerevisiae*. For expression of CaRad3 in yeast cells, the C-terminus 6x histidine tagged coding sequences of *C. albicans* orf19.7119 were amplified from genomic DNA of the BWP17 strain by PCR using primers (forward: 5′-CCG CAA GGA TCC ATG AAG TTC TTT ATT GAC GAC-3′, reverse: 5′-TAT CTC GAG TCA GTG GTG GTG GTG GTG GTG CAA CAA ATC TAA ATC CTC CTC ATC AAT ATC-3′). The 2325 bp of amplified DNA was digested with *Bam*HI and *Xho*I and inserted into the pESC(Ura) vector (Stratagene) restricted by *Bam*HI and *Sal*I. This construct was transformed into BY4741 using the lithium acetate method [26]. Transformed cells were pre-grown in selective synthetic medium with glucose as the carbon source at 30°C to an A_{600} of 0.8. Cells were collected by centrifugation and washed with chilled water. Cell pellets were resuspended and incubated in synthetic medium containing 2% galactose and 1% raffinose for expression of CaRad3 protein from the *GAL1* promoter. After 12 h, cells were collected via centrifugation and washed twice with chilled water and once with buffer A (50 mM Tris-HCl, pH 7.5, 150 mM NaCl, 0.1% NP-40, and 10% glycerol) containing 1 mM DTT and protease inhibitors (1 μg/ml pepstatin, 1 μg/ml PMSF, 5 μg/ml leupeptin, and 1 μg/ml aprotinin) and lysed with glass beads using the FastPrep-24 apparatus. Total lysates were centrifuged at 20,000*g* for 30 min at 4°C. Cleared lysates were loaded to the Ni-NTA column and purified as described above.

SDS-PAGE and western blotting. According to the manufacturer's instructions, purified proteins were analyzed by 10% SDS-PAGE gel for 3 h and visualized with Coomassie brilliant blue staining. Resolved recombinant proteins in SDS-PAGE were transferred to a nitrocellulose membrane using a semidry transfer kit overnight. After blocking for 1 h, each membrane was separately incubated for 1 h with a specific primary antibody in blocking buffer. Membranes were washed in washing buffer and then incubated with the secondary antibody for 1 h at room temperature. Following vigorous washing, antibody binding was visualized using the ECL detection system (GE Healthcare, USA) with X-ray film. Mouse anti-His antibody (Santa Cruz Biotechnology, USA) and mouse anti-Pgk1 (Molecular Probe, USA) were used as the primary antibodies in conjunction with a goat anti-mouse IgG-horseradish peroxidase-conjugated secondary antibody (Santa Cruz Biotechnology).

Assays for physical properties of the recombinant protein. The radius and molecular weight of CaRad3 were estimated by dynamic light scattering using a DynaPro-Titan instrument (Wyatt Technology, USA) at 22°C. Purified CaRad3 (2 mg/ml) in a freshly prepared buffer was filtered through a polyvinylidene difluoride filter (0.2 mm; Millipore). Scattering data were acquired through accumulation (5 times) of 10 scans at 10 sec/scan, with the laser intensity set to a range of 50-60% (30-36 mW). Corresponding molecular weight and radius were calculated using the DYNAMICS V6 software package supplied with the instrument. Electron magnetic resonance (EMR) analysis was performed to determine whether CaRad3 protein has a Fe-S cluster. The room temperature EMR spectrum was recorded with a JEOL JES-FA200 X-band (9.1-9.4 GHz) spectrometer. To prevent possible oxidation, powdered CaRad3 and a dried buffer powder (5 mg) were sealed in a 3-mm quartz EMR tube under $5 \cdot 10^{-5}$ torr. The microwave power was 1 mW,

and 5 G of AC magnetic modulation was used at 100 kHz. The time constant and gain were 0.03 sec and $5 \cdot 10^2$, respectively. For each sample, 16 signals were accumulated in the DC magnetic field ranging from 0 to 10,000 G for 32 min (2 min/scan). Finally, EMR signals from CaRad3 were corrected for background EMR signals obtained for both the empty EMR cell and the powdered buffer medium.

Helicase assay. For construction of 50 overhang DNA substrates, a 25-nt-long oligonucleotide (S25, sequence 5′-CCTCGAGGGATCCGTCCTAGCAAGC-3′) was 5′-[^{32}P]-end-labeled and annealed to the 3′ end of a 50-nt-long oligonucleotide (L50, sequence 5′-GCTCGAGTCTAGACTGCAGTTGAGAGCTTGCTAGGACGGATCCCTCGAGG-3′) by slow cooling from 85°C to room temperature and purified through G-25 columns (Amersham Biosciences). Helicase activity was assayed at 45°C in 25 mM MES (pH 6.5), 1 mM DTT, 0.1 mg/ml BSA, 20 nM ^{32}P-labeled DNA substrate, and 300 nM CaRad3 protein, and reactions were started by addition of a $MgCl_2$/ATP (1 mM final concentration). At specific time points (0, 30, and 60 min), 10 μl samples were taken and immediately added to 20 μl of chilled stop solution (10 mM Tris-HCl, pH 7.5, 5 mM EDTA, 5 mM competitor DNA (S25 oligo), 0.5% SDS, and 1 mg/ml proteinase K) and incubated for 20 min at room temperature to allow proteinase K digestion. Samples were separated on a native 12% acrylamide/TBE gel for 2 h at 130 V and quantified by phosphor imaging.

Functional analyses for the CaRad3 protein. Glycosidase assays were performed according to the manufacturer's instructions using peptide N-glycosidase F (PNGase F; NEB Inc.). Twenty micrograms of yeast cell lysates expressing the recombinant CaRad3 protein were combined with glycoprotein denaturing buffer (5% SDS, 0.4 M DTT) by a heating reaction at 100°C for 10 min. Denatured proteins were then incubated in 20 μl of G7 reaction buffer (0.5 M sodium phosphate, pH 7.5, 1% NP-40, 1 KU of PNGase F) at 37°C for 16 h. Deglycosylated samples were separated on a 10% SDS-PAGE gel and detected by western blotting with specific antibody for 6x histidine (Santa Cruz Biotechnology). For the complementation assay, subcloned CaRad3 was transformed into YR3-19 (rad3 Arg48) and YR3-57 ($rad3_{ts\text{-}14}$) mutant strains. As mentioned above, transformed cells were grown for expression of CaRad3 from the *GAL1* promoter in 2% galactose containing media. After 8 h, cells were collected by centrifugation and washed with PBS buffer. To determine whether CaRad3 affected RNA polymerase II transcription, galactose-induced transformed YR3-56 cells were streaked on YPAD and incubated at 25 or 39°C for 2 days. The UV sensitivity test was carried out essentially as previously described [27]. Transformed cells in YR3-19 were serially diluted in synthetic complete media and spotted on YPAD plates, which were irradiated with 0, 10, 20, and 30 J/m^2 of ultraviolet radiation, respectively, and immediately placed in the dark at 30°C for 3 days. Each phenotype test was carried out more than three times with three different colonies.

RESULTS

Isolation and characterization of putative *CaRad3 orf19.7119* gene. The genome of the fungal pathogen *C. albicans* has been completely sequenced [28]. The putative *Rad3* (*orf19.7119*) sequence was obtained by searching the *Candida* Genome Database (http://www.candidagenome.org). Based on the sequence information, specific primers for the gene were designed and used for PCR using genomic DNA. The genomic DNA of *orf19.7119* was 2298 bp long without difference between the candida genome assemblies 19 and 21. This sequence corresponds to a protein of 765 amino acid residues with a predicted molecular weight of approximately 90 kDa. Figure 1 shows a multiple alignment of the amino acid sequence of putative CaRad3 with those of Rad3 enzymes from various species. CaRad3 showed a sequence identity of 77.4, 52.7, 48.6, and 19.8% with Rad3 (or XPD) of *S. cerevisiae*, *H. sapiens*, *A. thaliana*, and *S. acidocaldarius*, respectively. CaRad3 has a conserved domain positioned near the N-terminus between helicase motifs I and II, similar to other eukaryotic Rad3 family members [29]. The key characteristic of this domain is the conservation of four cysteine residues, suggestive of a metal ion-binding motif. This motif is present at an equivalent position to the hairpin domain of the bacterial NER helicase UvrB, which serves to physically separate DNA strands [30]. Good sequence alignment of CaRad3 with other Rad3 members suggests that they may have similar characteristics.

Expression and purification of recombinant CaRad3 protein in *E. coli*. We constructed the bacterial expression vector for 6x histidine tagged CaRad3 protein as described in the "Materials and Methods" section. When we experimentally initiated a project to establish a bacterial expression system for CaRad3, the expressed level of eukaryotic recombinant CaRad3 was very low in typical LB media, and most of the expressed proteins were in insoluble aggregates. In subsequent experiments, several alterations of the expression protocol were directed at increasing the amount of soluble protein. Bacterial acclimation to osmotic stress involves intracellular accumulation, by synthesis or uptake, of osmolytes that equilibrate cellular osmotic pressure. *In vitro*, osmolytes such as glycine betaine, proline, or glycerol may protect native proteins from heat denaturation and favor formation of native proteins. Some osmolytes also behave as "chemical chaperones" by promoting the correct folding of unfolded proteins *in vitro* and *in vivo* [31, 32]. In pursuing the expression of CaRad3, we submitted transformants of *E.*

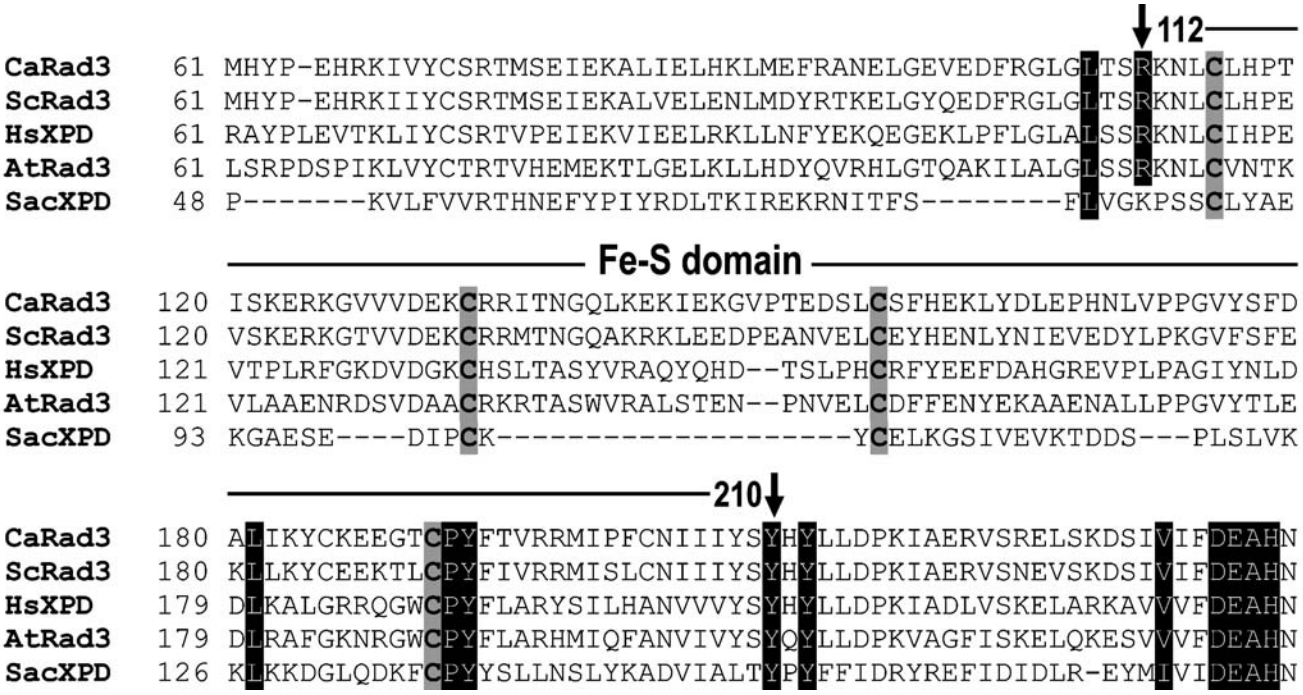

Fig. 1. Sequence alignment of the region between helicase motifs I and II, including the Fe-S domain, for human and yeast helicases. HsXPD, human XPD; ScRad3, *S. cerevisiae* Rad3; CaRad3, *C. albicans* Rad3; AtRad3, *A. thaliana* Rad3; SacRad3, *S. acidocaldarius* Rad3. The four conserved cysteine residues in the Fe-S cluster are in bold in gray. Canonical helicase motifs are indicated in black.

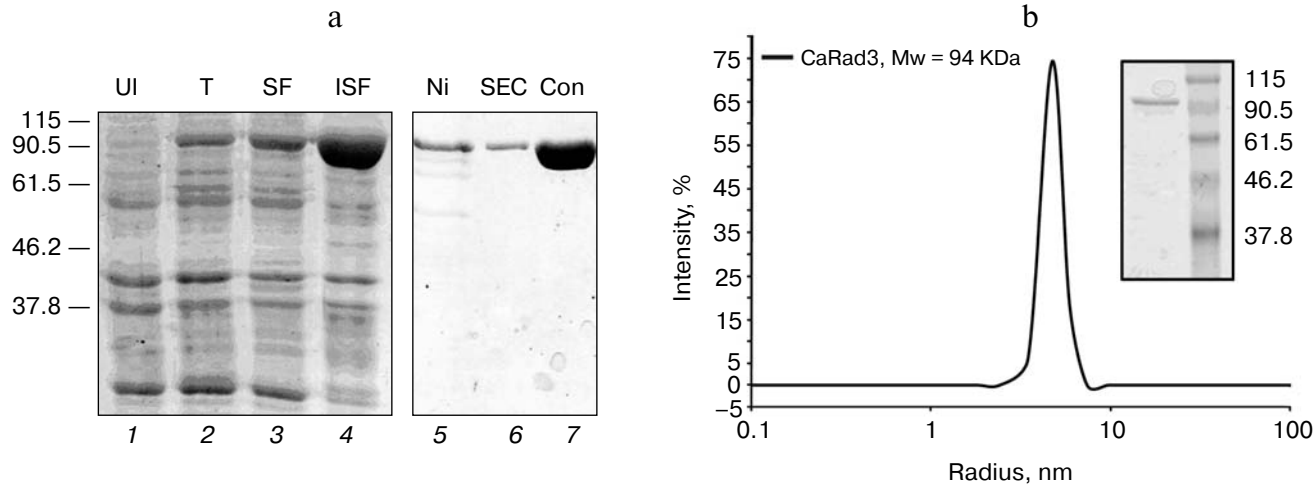

Fig. 2. Monomeric status of purified CaRad3 proteins. a) SDS-PAGE was performed on 10% gel and stained with Coomassie Brilliant Blue. Expression (left panel) and purification (right panel) of recombinant CaRad3 in bacteria: lanes: *1*) (UI) non-induced whole-cell lysates; *2*) (T) induced whole-cell lysates; *3*) (SF) soluble fraction of induced cells; *4*) (ISF) insoluble fraction of induced cells; *5*) (Ni) elution from Ni-affinity resin; *6*) (SEC) elution from a size exclusion column; *7*) (Con) concentrated purified CaRad3. b) Molecular mass determination of CaRad3 in solution and dynamic light scattering data for CaRad3 (2 mg/ml). The calculated molecular radius and molecular weight of CaRad3 are 4.02 nm and 94 kDa, respectively, indicating its monomeric nature. The inset shows an SDS-PAGE gel of the purified CaRad3 protein.

coli strains ER2566 to a pre-adaptation with the osmolyte sorbitol in an overnight culture and used these cells for inoculation of an "expression culture" with sorbitol. Following induction with IPTG (0.1 mM), we examined lysis supernatants (soluble protein) as well as pelleted cell debris (insoluble protein). Consequently, CaRad3 was expressed at high levels in *E. coli* in modified culture media containing the osmolyte sorbitol (YEP medium

containing 0.2 M sorbitol), and the amount of pure recombinant CaRad3 protein was approximately 10 mg/ml (Fig. 2a). For measurement of the molecular weight and radius of purified CaRad3 proteins, we used a technique in physics known as dynamic light scattering. As expected from the open reading frame of the gene, the purified CaRad3 gave a single band on SDS-PAGE at 94 kDa. Purified CaRad3 was studied by light scattering to determine its tendency to form oligomer. Dynamic light scattering experiments clearly indicated the monomeric nature of CaRad3, with a calculated molecular radius and translated molecular weight of CaRad3 of 4.02 nm and 94 kDa, respectively, in solution at 2 mg/ml, as indicated in three recent reports on the crystal structure of archaeal XPDs (PDB ID: 3CRW, 2VL7, and 2VSF) (Fig. 2b) [33-35].

Physicochemical characterization of recombinant CaRad3 protein. The UV-visible absorption spectrum was measured for analysis of the physicochemical properties of CaRad3 protein. The heterogeneously expressed CaRad3 protein in *E. coli* had a light yellow-green color with absorbance maxima at 330 and 420 nm and broad shoulders at 460 and 570 nm (Fig. 3a). Upon storage under anoxic conditions for several days, the major part of the absorbance was irreversibly lost, which indicated cluster breakdown (Fig. 3a, inset). These observations suggested the presence of a Fe-S cluster in CaRad3. In subsequent experiments, existence of an iron species can be confirmed by electron magnetic resonance (EMR) spectroscopy (Fig. 3b). The darkest line of Fig. 3b shows the EMR spectrum obtained for a wild type of CaRad3. At first glance, two strong peaks were observed; one was an extraordinarily broad peak ($g > 10$), and the other was a relatively narrow one at 3197 G ($g = 2.04$). Additional weak peaks were also seen at $g = 2.5$ (2645 G) and $g = 4.7$ (1381 G), respectively. Considering its g-value, the weak peaks of $g = 4.7$ and 2.5 were probably due to the presence of a Fe^{3+} ($S = 3/2$) ion under octahedral symmetry and a ligand-free Fe^{3+} ($S = 1/2$) ion, respectively. In addition, it should be noted that two strong peaks greatly resembled the EMR spectrum from the powdered *E. coli* endonuclease III containing iron-sulfur [4Fe-4S] cofactor in our previous study [36]. On paper, the extraordinarily broad EMR peak of $g > 10$ was interpreted as a non-resonant microwave absorption caused by fluctuations of electric dipole moments established between Fe^{2+} and Fe^{3+} in the [4Fe-4S] cluster [36]. In this sense, CaRad3 is said to contain an iron-sulfur cluster as well. To reconfirm this scenario, oxidized and reduced CaRad3 samples were prepared and then measured using EMR spectroscopy. Two gray lines in Fig. 3b show the EMR results. Of particular interest, intensive decreases in EMR intensities were observed, particularly for the non-resonant microwave absorption peak. Such responses were possible only when there was either a structural change or a variation in valence state of the iron-sulfur cluster. The EMR peak caused by the Fe^{3+} ion with an octahedral symmetry peak of $g = 4.7$ was shifted to $g = 4.2$. Furthermore, EMR peaks observed at $g = 2.5$ and 2.04 had almost the same g-values; however, their relative intensities were slightly varied. In particular, for the reduced CaRad3, the EMR peak of g =

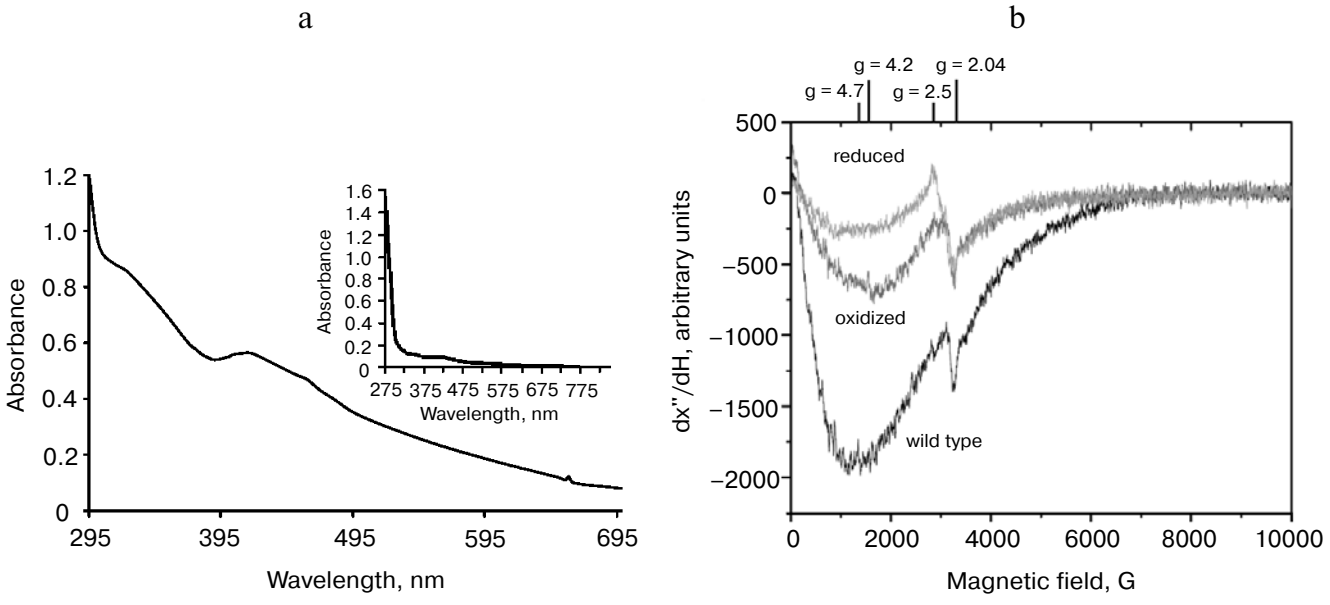

Fig. 3. CaRad3 contains a Fe-S cluster. a) UV-Vis absorption spectrum of CaRad3 produced in *E. coli*. The inset shows the spectrum of CaRad3 after storage for 10 days. b) Electron magnetic resonance signals obtained for wild (black), oxidized (gray), and reduced (gray) types of CaRad3 specimens at room temperature. Each vertical bar indicates spectroscopic g-factors. Instrumental conditions: microwave power, 1 mW; AC magnetic field modulation, 5 G; receiver gain, $5 \cdot 10^2$; total accumulation, 16 times.

4.2 disappeared, and the g = 2.5 peak showed a simultaneous increase, despite the fact that g = 2.04 remained constant. This may be related to an effective chelating of the Fe^{3+} under octahedral symmetry by the reducing agent. It can be conclusively suggested that CaRad3 has an iron-sulfur cluster.

ATP-dependent helicase activity of CaRad3. To determine whether putative CaRad3 is indeed a helicase, we analyzed unwinding of partially duplex DNA substrates. The 5′-overhang 50-nucleotide duplex substrates were used with bacterially expressed CaRad3 in a helicase assay with or without ATP. As expected, purified CaRad3 was able to function as an ATP-dependent 5′-3′ DNA helicase, displacing a DNA strand from partially duplex DNA substrates (Fig. 4). Because the helicase activity of *S. acidocaldarius* Rad3 is sensitive to the integrity of the Fe-S cluster [29], we disrupted this cluster with a metal-ion chelator. CaRad3 without Fe by adding of EDTA showed almost complete loss of helicase activity even in the presence of ATP (Fig. 4b, lane 10). ATP hydrolysis is therefore uncoupled from strand displacement in CaRad3 lacking the Fe-S cluster. These results showed that the product of *orf19.7119* genes (CaRad3) has real ATP-dependent helicase activity and also implied that the Fe-S cluster of CaRad3 is essential for DNA strand displacement by the enzyme. However, mechanistic details for the coupling of ATP hydrolysis to strand displacement are not well understood through this experiment.

Glycosylation of recombinant CaRad3 purified from *S. cerevisiae*. The NetNGlyc1.0 (http://www.cbs.dtu.dk/services/NetNGlyc/) [37] server was used for prediction of putative N-linked glycosylation sites (Fig. 5a). If we assume that the topology of CaRad3 is similar to that of archaeal XPD, the only glycosylation site would be predicted at asparagine 701 (701-NDSD-704) with high probability [29]. To investigate this post-translational modification, recombinant CaRad3 protein, which was driven from an inducible *GAL1* promoter, was expressed in *S. cerevisiae*. This fungal system enabled modification and overexpression of CaRad3 protein by galactose induction. We constructed the 6x histidine tagged CaRad3 in yeast expression vector pESC(URA) (Invitrogen) as described in the "Materials and Methods" section. Transformed yeast cells with recombinant

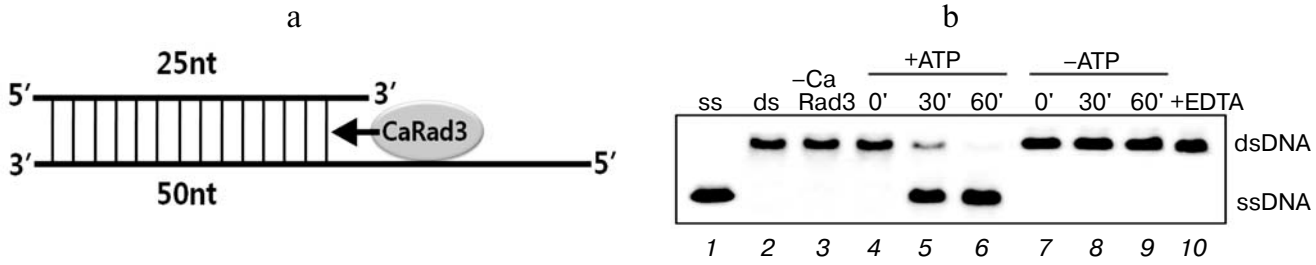

Fig. 4. Helicase activities of CaRad3. a) Schematic of the helicase assay and substrate design. b) CaRad3 is an ATP-dependent DNA helicase. The displaced DNA strand accumulates over time upon incubation at 45°C. EDTA was added to chelate iron ions. There is no strand displacement in the absence of ATP or CaRad3 or in the presence of EDTA. The reaction time used and whether ATP was present or not is indicated at the top of each panel.

a

Position	Sequence	Potential	N-Glyc result
701	NDSD	0.5961	+
706	NLST	0.3659	-

691-QLPKWIAQAL **NDSD**T**NLST**D MALATAKKFL-720

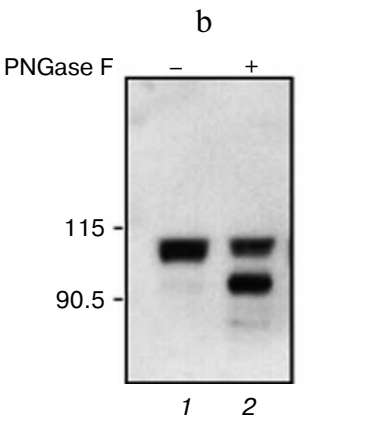

Fig. 5. N-Glycosylation of recombinant CaRad3 protein. a) Estimation of N-glycosylation site with high probability using NetNGlyc 1.0. The table shows predicted N-glycosylation sites in amino acid sequences of CaRad3. N-Glycosylation potential (0.5) is taken as a cutoff. b) CaRad3 was found to be glycosylated, as revealed by protein-band shifts upon digestion of 1 μg of His-CaRad3 expressed in yeast with 10 units of PNGase F. Immunoblotting was performed using anti-His antibody.

CaRad3 were induced by 2% galactose, and cleared whole cells extracts were loaded onto a Ni-NTA column. Following elution of the His-tagged proteins by imidazole, the appropriated fractions were pooled. However, due to a low level of expression, the purified CaRad3 protein could not be visualized by Coomassie brilliant blue staining. Instead, we attempted its detection using western blotting with specific antibody for 6x histidine. As shown in Fig. 5b (lane *1*), a protein that was relatively larger in size than the bacterially expressed form was observed. Based on the fact that CaRad3 encodes consensus sites for glycosylation, we speculated that the 100 kDa band might be due to N-linked glycosylation. When cell lysates from CaRad3-expressing yeast cells were treated with PNGase F, the migrating CaRad3 species accumulated into the 94 kDa species, strongly suggesting that the presence of the band with higher than expected molecular weight in CaRad3-expressing cells was due to N-linked glycosylation (Fig. 5b). Our data indicate that at least CaRad3 is glycosylated, which is not a common phenomenon in nuclear proteins.

Functional complementation of CaRad3 to defective ScRad3. Previous studies revealed that *S. cerevisiae* Rad3, an ortholog of CaRad3, has a pivotal role in nucleotide excision repair, transcription, and recombination [38-40]. Mutation of lysine-48 to arginine in the ScRad3 protein abolishes its ATPase and DNA helicase activities, but not its ability to bind ATP [41]. In addition, this mutation confers a substantial reduction in cell viability when cells are irradiated with ultraviolet radiation. To determine whether CaRad3 complements the viability and DNA repair defects of ScRad3 mutant (rad3Arg48) cells, we evaluated the UV sensitivity of rad3Arg48 mutant cells harboring CaRad3. CaRad3 protein, which was driven from an inducible *GAL1* promoter, was ectopically expressed in galactose media and subjected to UV sensitivity analysis (Fig. 6a). Expression of CaRad3 protein from the mutant strain was verified by western blotting (Fig. 6b). The rad3Arg48 strain carrying the CaRad3 gene showed increased cell viability, which was much better than that of the wild type strain. To eliminate the possibility that ectopically overexpressed proteins induced unexpected artifactual effects, rad3Arg48 cells harboring the *CaRad3* gene were grown only in 2% glucose synthetic minimal media without induction and were also subjected to UV sensitivity analysis. These cells also showed increased cell viability, as shown in cells induced by galactose. These results implied that CaRad3 could substitute for ScRad3 required for UV damaged DNA repair. Another ScRad3 mutant strain, $rad3_{ts\text{-}14}$, is defective in mRNA synthesis by RNA polymerase II, which is not grown at 39°C, a non-permissive temperature [21]. To determine whether CaRad3 is involved in RNA polymerase II transcription, CaRad3 was also introduced into the $rad3_{ts\text{-}14}$ mutant strain and cultivated at the non-permissive temperature (39°C). CaRad3 carrying $rad3_{ts\text{-}14}$ cells restored normal growth at the non-permissive temperature (Fig. 6c). This observation indicated that CaRad3 is essential for transcription by RNA polymerase II. Taken together with the above data, we concluded that CaRad3, an ortholog of *S. cerevisiae* Rad3, plays physiological roles in transcription and DNA repair with ATPase and helicase activity.

DISCUSSION

Recently, ROS generation of macrophages has been one of the issues in infection of *Candida albicans* as a phagocyte-mediated host response [15, 16]. These toxic compounds induce DNA damage on the chromosomes of invasive pathogens and further activate defensive signaling pathways in host organisms [14]. To escape and survive from attack by phagocytes, *C. albicans* developed a system of evasion for scavenging of ROS and repair of damaged DNA [14]. NER is thought to be a guardian in maintenance of genome integrity. It is also a key modulation step in acquisition of resistance to antifungal drugs. The mortality rate associated with disseminated infection approaches 40% due to increased resistance to most antifungal drugs, including polyenes (amphotericin B), azole (fluconazole), and echinocandins (caspofungin) [4]. Increased resistance to the available antifungal drugs was obtained by genetic modifications, such as point mutations of specific drug target genes and chromosomal rearrangements [42, 43].

In this study, we have cloned the *Candida Rad3* gene in a major component of NER and expressed recombinant CaRad3 protein in both prokaryote and eukaryote. Changes in culture media provide a means for isolation of large quantities of highly purified CaRad3 protein in relatively uniform and low aggregation state, which can easily be concentrated to greater than 5 mg protein/ml without the use of any ingredients (Fig. 2). It is hoped that the benefits derived from this modification will facilitate their structural studies, such as NMR and X-ray crystallography. We have also characterized the physicochemical properties of purified CaRad3 protein as a member of the Rad3 family. DNA helicases of the Rad3 family possess a unique structural domain inserted between helicase signature motifs Ia and II. This element contains an unusual structure, a Fe-S cluster [29]. Our EMR and spectrometric analyses indicated that CaRad3 protein has a Fe-S cluster, similar to that of archaeal XPD (Fig. 3). CaRad3 displays helicase activity on partially duplex DNA substrates (Fig. 4). Monomeric helicases are thought to catalyze strand displacement by an "inchworm" mechanism that requires separate domains responsible for ATP-dependent tracking along single strand DNA and for destabilization of duplex DNA [44]. The Fe-S cluster in CaRad3 therefore defines a domain that serves to separate

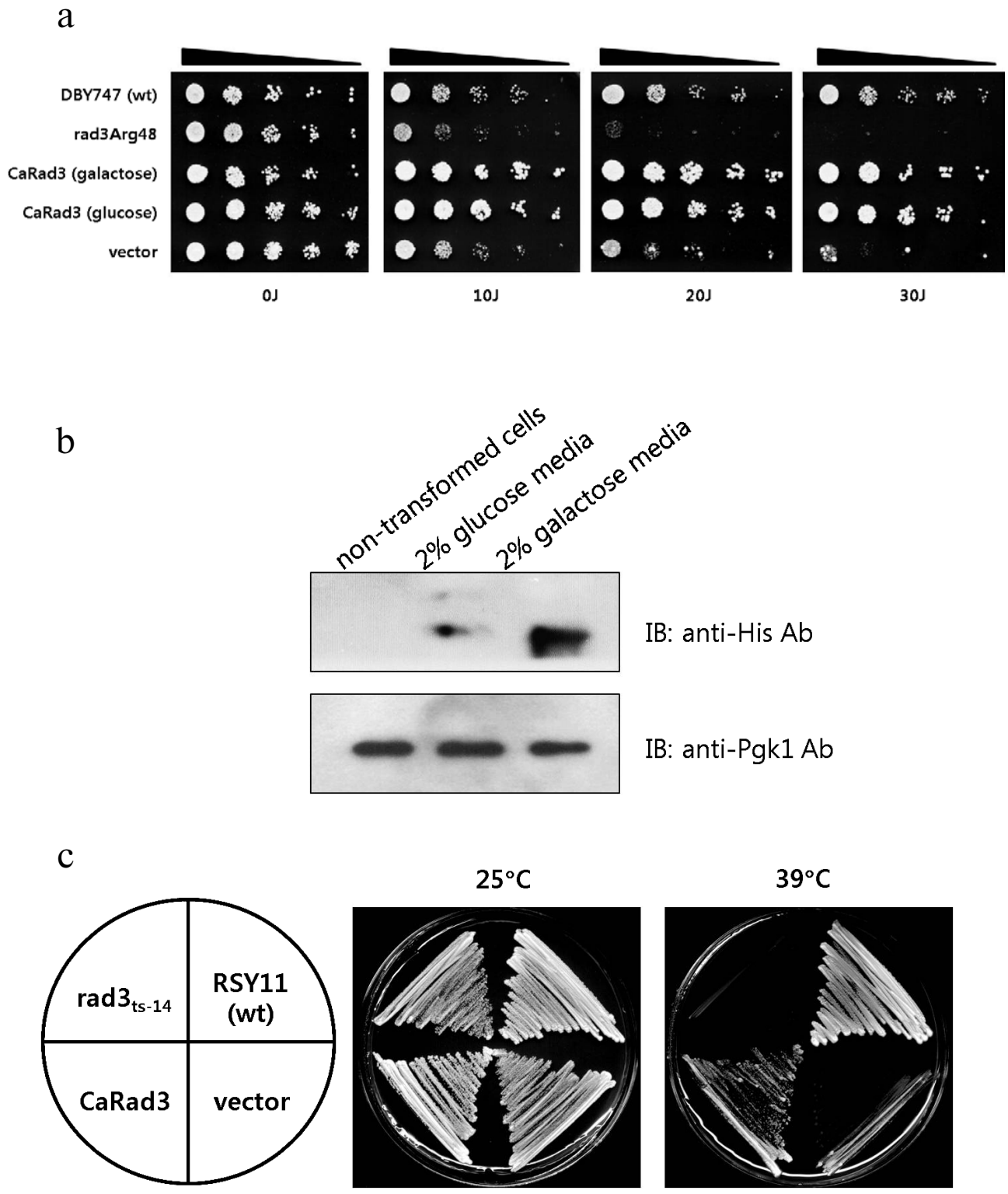

Fig. 6. Complementation of CaRad3 for defective ScRad3 mutant strains. a) Rad3Arg48 cells are defective in helicase and ATPase. Cells transformed with CaRad3 were evaluated for cell viability after UV irradiation. b) Expression of CaRad3 protein was verified with western blotting with a specific antibody for 6x histidine using whole cell extracts. CaRad3 protein was faintly observed without induction by galactose. Pgk1 was used as an internal control. c) Temperature sensitive mutant $rad3_{ts\text{-}14}$ cells, which are defective in transcription of RNA polymerase II, cannot grow at the non-permissive temperature (39°C). Transformed cells with CaRad3 were compared with wild type cells using cells viability at the non-permissive temperature.

DNA strands as the protein translocates along DNA. In addition, it is possible that the Fe-S cluster in the Rad3 family helicases is the important site for the coupling of ATP hydrolysis with conformational changes necessary for strand displacement. For example, as ATP is bound, hydrolyzed, and ADP released, cyclical changes in the redox state of the cluster could generate local changes in protein conformation. This means that CaRad3 can modify helicase activities or confer specificity for a defined set of DNA structures through this auxiliary domain containing the Fe-S cluster. Additionally, we demonstrated that recombinant CaRad3 protein was N-glycosylated, as revealed by treatment with PNGase F. There are few known glycosylated nuclear proteins, especially DNA repair proteins. Glycosylation is one of the post-translational modifications that can produce significant structural changes in proteins. Depending on the structure of the attached glycans, glycosylation of proteins provides various functions, such as protein folding, stability, degradation, signaling, and cell communication [45]. Functional characterization of the glycosylation of CaRad3 could be another important topic in the DNA repair mechanism and pathogenesis of *C. albicans*. Finally, we found that CaRad3 protein functionally complemented the defects in NER and transcription of ScRad3. Taken together, these findings suggest that CaRad3 is an ortholog of ScRad3. However, to determine the physiological role of CaRad3 in *Candida albicans*, we should construct conditional knock-out strains for the *CaRad3* gene, which is an essential gene for survival, and diverse genetic and toxicological approaches should be further attempted with regard to survival analysis to macrophage or antifungal drugs using these mutant strains.

We are grateful to Dr. S. Prakash and Dr. L. Prakash (University of Texas Medical Branch, Texas) for their generous gift of the ScRad3 mutant strains.

This work was supported by the Bio-Scientific Research Grant funded by the Pusan National University (PNU, Bio-Scientific Research Grant) (PNU-20080599000).

REFERENCES

1. Giglia-Mari, G., Coin, F., Ranish, J. A., Hoogstraten, D., Theil, A., Wijgers, N., Jaspers, N. G., Raams, A., Argentini, M., van der Spek, P. J., Botta, E., Stefanini, M., Egly, J. M., Aebersold, R., Hoeijmakers, J. H., and Vermeulen, W. (2004) *Nat. Genet.*, **36**, 714-719.
2. Liu, Z., Hong, S. W., Escobar, M., Vierling, E., Mitchell, D. L., Mount, D. W., and Hall, J. D. (2003) *Plant Physiol.*, **132**, 1405-1414.
3. Hanawalt, P. C., Ford, J. M., and Lloyd, D. R. (2003) *Mutat. Res.*, **544**, 107-114.
4. Legrand, M., Chan, C. L., Jauert, P. A., and Kirkpatrick, D. T. (2007) *Eukaryot. Cell*, **6**, 2194-2205.
5. Navarro, M. S., Bi, L., and Bailis, A. M. (2007) *Genetics*, **176**, 1391-1402.
6. Lehmann, A. R. (2003) *Biochimie*, **85**, 1101-1111.
7. Lehmann, A. R. (2001) *Genes Dev.*, **15**, 15-23.
8. Graham, J. M., Jr., Anyane-Yeboa, K., Raams, A., Appeldoorn, E., Kleijer, W. J., Garritsen, V. H., Busch, D., Edersheim, T. G., and Jaspers, N. G. (2001) *Am. J. Hum. Genet.*, **69**, 291-300.
9. Scharer, O. D. (2008) *DNA Repair (Amst.)*, **7**, 339-344.
10. Bootsma, D., and Hoeijmakers, J. H. (1993) *Nature*, **363**, 114-115.
11. Coin, F., Oksenych, V., and Egly, J. M. (2007) *Mol. Cell*, **26**, 245-256.
12. Winkler, G. S., Araujo, S. J., Fiedler, U., Vermeulen, W., Coin, F., Egly, J. M., Hoeijmakers, J. H., Wood, R. D., Timmers, H. T., and Weeda, G. (2000) *J. Biol. Chem.*, **275**, 4258-4266.
13. Pugh, R. A., Honda, M., Leesley, H., Thomas, A., Lin, Y., Nilges, M. J., Cann, I. K., and Spies, M. (2008) *J. Biol. Chem.*, **283**, 1732-1743.
14. Netea, M. G., Brown, G. D., Kullberg, B. J., and Gow, N. A. (2008) *Nat. Rev. Microbiol.*, **6**, 67-78.
15. Wellington, M., Dolan, K., and Krysan, D. J. (2009) *Infect. Immun.*, **77**, 405-413.
16. Frohner, I. E., Bourgeois, C., Yatsyk, K., Majer, O., and Kuchler, K. (2009) *Mol. Microbiol.*, **71**, 240-252.
17. Alao, J. P., and Sunnerhagen, P. (2008) *Mol. Microbiol.*, **68**, 246-254.
18. Singh, R. K., and Krishna, M. (2006) *Mol. Cell. Biochem.*, **290**, 103-112.
19. Matsuura, A., Naito, T., and Ishikawa, F. (1999) *Genetics*, **152**, 1501-1512.
20. Bailis, A. M., Maines, S., and Negritto, M. T. (1995) *Mol. Cell. Biol.*, **15**, 3998-4008.
21. Guzder, S. N., Qiu, H., Sommers, C. H., Sung, P., Prakash, L., and Prakash, S. (1994) *Nature*, **367**, 91-94.
22. Deschavanne, P. J., and Harosh, I. (1993) *Mol. Microbiol.*, **7**, 831-835.
23. Reynolds, P. R., Biggar, S., Prakash, L., and Prakash, S. (1992) *Nucleic Acids Res.*, **20**, 2327-2334.
24. Harosh, I., Naumovski, L., and Friedberg, E. C. (1989) *J. Biol. Chem.*, **264**, 20532-20539.
25. Sherman, F. (2002) *Meth. Enzymol.*, **350**, 3-41.
26. Gietz, R. D., Schiestl, R. H., Willems, A. R., and Woods, R. A. (1995) *Yeast*, **11**, 355-360.
27. Stitzel, M. L., Durso, R., and Reese, J. C. (2001) *Genes Dev.*, **15**, 128-133.
28. Jones, T., Federspiel, N. A., Chibana, H., Dungan, J., Kalman, S., Magee, B. B., Newport, G., Thorstenson, Y. R., Agabian, N., Magee, P. T., Davis, R. W., and Scherer, S. (2004) *Proc. Natl. Acad. Sci. USA*, **101**, 7329-7334.
29. Rudolf, J., Makrantoni, V., Ingledew, W. J., Stark, M. J., and White, M. F. (2006) *Mol. Cell.*, **23**, 801-808.
30. Skorvaga, M., Theis, K., Mandavilli, B. S., Kisker, C., and van Houten, B. (2002) *J. Biol. Chem.*, **277**, 1553-1559.
31. Diamant, S., Eliahu, N., Rosenthal, D., and Goloubinoff, P. (2001) *J. Biol. Chem.*, **276**, 39586-39591.
32. Frings, E., Sauer, T., and Galinski, E. A. (1995) *J. Biotechnol.*, **43**, 53-61.
33. Fan, L., Fuss, J. O., Cheng, Q. J., Arvai, A. S., Hammel, M., Roberts, V. A., Cooper, P. K., and Tainer, J. A. (2008) *Cell*, **133**, 789-800.

34. Liu, H., Rudolf, J., Johnson, K. A., McMahon, S. A., Oke, M., Carter, L., McRobbie, A. M., Brown, S. E., Naismith, J. H., and White, M. F. (2008) *Cell*, **133**, 801-812.
35. Wolski, S. C., Kuper, J., Hanzelmann, P., Truglio, J. J., Croteau, D. L., van Houten, B., and Kisker, C. (2008) *PLoS Biol.*, **6**, e149.
36. Kim, S. H., Kim, H. D., Youn, B., Lee, C. H., and Kim, J. (2008) *J. Korean Phys. Soc.*, **52**, 1065-1069.
37. Blom, N., Sicheritz-Ponten, T., Gupta, R., Gammeltoft, S., and Brunak, S. (2004) *Proteomics*, **4**, 1633-1649.
38. Bailly, V., Sung, P., Prakash, L., and Prakash, S. (1991) *Proc. Natl. Acad. Sci. USA*, **88**, 9712-9716.
39. Sung, P., Prakash, L., Weber, S., and Prakash, S. (1987) *Proc. Natl. Acad. Sci. USA*, **84**, 6045-6049.
40. Sung, P., Prakash, L., Matson, S. W., and Prakash, S. (1987) *Proc. Natl. Acad. Sci. USA*, **84**, 8951-8955.
41. Sung, P., Higgins, D., Prakash, L., and Prakash, S. (1988) *EMBO J.*, **7**, 3263-3269.
42. Dunkel, N., Liu, T. T., Barker, K. S., Homayouni, R., Morschhauser, J., and Rogers, P. D. (2008) *Eukaryot. Cell*, **7**, 1180-1190.
43. Selmecki, A., Forche, A., and Berman, J. (2006) *Science*, **313**, 367-370.
44. Soultanas, P., Dillingham, M. S., Wiley, P., Webb, M. R., and Wigley, D. B. (2000) *EMBO J.*, **19**, 3799-3810.
45. Lauc, G., Rudan, I., Campbell, H., and Rudd, P. M. (2010) *Mol. Biosyst.*, **6**, 329-335.